ELSEVIER

Biophysical Chemistry 88 (2000) 69–80

Biophysical Chemistry

www.elsevier.nl/locate/bpc

Structural constraints regulating triple helix formation by A-tracts

Anjana Sen, Astrid Gräslund*

Department of Biophysics, Arrhenius Laboratories, Stockholm University, S-106 91 Stockholm, Sweden

Received 19 June 2000; accepted 15 August 2000

Abstract

The study concerns the propensity of triple helix formation by different DNA oligonucleotides containing long A-tracts with and without flanking G·C base pairs in order to probe the role of length of the A-tract and the flanking sequences. From nuclear magnetic resonance (NMR) studies of imino proton spectra and circular dichroism (CD) spectroscopy of samples composed of potential triplex forming strand sequences in correct stoichiometries, we have concluded that 8-mer A-tracts flanked by G·C base pairs exert significant steric hindrance to triple helix formation. When as much as 50 mM Mg^{2+} was added, no triple helix formation was observed in these samples. In contrast, open-ended 8-mer A-tracts formed triplex with the corresponding two T_8 strands under relatively mild ionic conditions (100 mM Na^+). Moreover, the shorter the length of the A-tract, the less is the hindrance to form a triple helix.

Keywords: Triple helix; A-tract; Nuclear magnetic resonance; Circular dichroism

1. Introduction

A-tracts may be defined as double-stranded 4–8 A·T base-paired DNA segments without interruption by a TpA step. They exhibit a narrowed minor groove, strong propeller-twisted base pairs and deviation from the normal C2′-endo sugar puckering. The anomalous structural features of A-tracts have been reviewed by Crothers et al. [1]. Since the discovery by Crothers' group and other reports on A-tract bending [2–5], several investigations exploring its special structural features have been performed by different research groups [6–8].

DNA is a conformationally flexible molecule that can adopt several types of non-B structural motifs including multi-strand helices, among

Abbreviations: W–C, Watson–Crick; H-bond, hydrogen bond; Pyr, pyrimidine; Pur, purine; TSP, 3-(trimethylsilyl) tetradeutero sodium propionate

* Corresponding author. Tel: +46-8-162-450; fax: +46-8-155-597.

E-mail address: astrid@biophys.su.se (A. Gräslund).

0301-4622/00/$ - see front matter
PII: S0301-4622(00)00200-3

which DNA triple helices have drawn increasing attention in recent years [9–17], (for review see Shafer [18]) due to their potential role in inhibition of transcription, mediating mutagenesis and in antigene drug therapy as well as their importance in biotechnological applications [12,19,20]. In the early 1990s, oligonucleotide-directed triple helix formation came to focus with the biochemical and medical applications of its versatile nature of sequence specific recognition [19,21] (and references therein).

The two major nucleic acid triple helix motifs with Hoogsteen or reverse Hoogsteen base pairing of a third strand with a DNA double helix have been defined. They include numerous ways of third strand association depending on the sequences of the host duplex and the third strand itself that makes it complicated in terms of polarity rules and specificity. In the Pyr·Pur*Pyr type triplet motif, the purine strand in the middle position forms W–C type hydrogen bonds with one of the two pyrimidine strands in an antiparallel sense and the second pyrimidine strand running parallel to this purine strand forming normal Hoogsteen type H-bonds. In the other triplet motif, Pyr·Pur*Pur, the second purine strand runs antiparallel to the other purine strand which is, on the other side, engaged in W–C type base pairing and in this case Pur*Pur H-bonds are reverse Hoogsteen type. In the triplexes, extra screening of phosphate anionic charge repulsion is necessary, especially in the former case where two parallel chains in the Hoogsteen part show higher phosphate–phosphate anionic charge repulsion due to a closer proximity [9]. Therefore, triplex formation is associated with three major criteria: (a) the participating strand sequences must be of homopurine/homopyrimidine type; (b) triplex formation is favored by the presence of divalent cations, while only the monovalent cations are generally enough for the W–C H-bond formation; (c) Hoogsteen type H-bond formation allows degeneracy regarding the third strand DNA sequence, i.e. either a homopyrimidine or a homopyrimidine strand may bind as the third strand but with different polarity rules.

Our investigation deals with the sequence-related regulating factors of the triple helix forming capability of model oligonucleotide systems. We have used mainly nuclear magnetic resonance (NMR) to study how the length of a homoadenine sequence and the sequences of its surrounding segments influence its ability to take part in triple helix formation. The ability to take part in triple helix formation has been related to the structural characteristics of the sequence. We have found that a duplex where G·C base pairs surround an A_8/T_8 segment displaying some typical characteristics of an A-tract, is unable to form a triplex with an added $d(T)_8$ strand even at high divalent cation concentration (50 mM Mg^{2+}). However, an 8-mer homoadenine strand without surrounding G·C base pairs forms a triple helix with two 8-mer homothymine strands under relatively mild ionic conditions. The relation between the A-tract structural characteristics and the ability to form DNA triple helices is discussed.

2. Materials and methods

2.1. Chemicals and oligodeoxynucleotides

All chemicals used were of analytical grade. The single stranded oligonucleotides d(CGCA_8CGC), d(GCGT_8GCG), $d(A)_6$, $d(T)_6$, $d(A)_8$, $d(T)_8$ were purchased from either CyberGene AB, Sweden or DNA Technology A/S, Denmark and used without further purification. Stock solutions were prepared by dissolving them in 10 mM phosphate buffer (pH 7.2). Circular dichroism (CD) samples were prepared by dilution of stock solutions with required amount of added salt and NMR samples with also 1 mM EDTA and 10% D_2O/90% H_2O. NaCl and EDTA used in NMR samples were Ultra-Pure grade from Sigma. The strand concentration for CD samples was 6 μM and for NMR it was in the range of 0.5–2 mM.

2.2. Circular dichroism

Equimolar solutions (6 μM) of the oligonucleotide strands in 10 mM phosphate buffer (pH 7.2), with required amounts of salt were combined

to give appropriate stoichiometries. The ellipticities of those mixtures as well as of the individual single strands were measured in the range of 200–350 nm in a Jasco J-720 spectropolarimeter. The temperature was held at 1°C or 5°C by using a PTC-343 temperature programmer and controller.

2.3. Imino proton NMR

NMR experiments were performed either with a 400 or a 600 MHz Varian Inova spectrometer. Imino proton measurements were made on 500 μl samples in 10 mM phosphate buffer with required amount of salt, 1 mM EDTA, 0.1 mM TSP and 10% D_2O/90% H_2O. Sigma Ultra-Pure reagents were used to make NMR samples. Chemical shift values are set with respect to the TSP as an internal standard. The imino proton spectra were recorded using a Jump-Return sequence for solvent suppression with the carrier frequency set at the H_2O resonance. An interval delay of 49 μs was used along with a pulse repetition time of 2 s.

3. Results

Fig. 1 depicts three schemes of possible DNA base triplets consisting of both W–C and Hoogsteen type H-bonding. W–C base paired strands containing A·T and G·C base pairs run antiparallel to each other. The first triplet (top) is a Pyr·Pur*Pyr motif where Hoogsteen base paired strands containing A*T base pairs run parallel to each other. In the second (middle) and third (bottom) triplets, reverse Hoogsteen base paired strands containing G*G and A*A base pairs run antiparallel to each other forming Pyr·Pur*Pur motifs. In the NMR spectroscopic study, the presence of W–C and Hoogsteen base pairs and triplets are clearly evidenced by the appearance of T imino proton resonances which are observable due to the slow exchange of the H-bonded protons.

We have studied the triplex formation propensities of A_8/T_8 tracts with different flanking sequences and also without any flanks, as well as the dependence of the triplex-forming propensity on the length of the A_n/T_n tract.

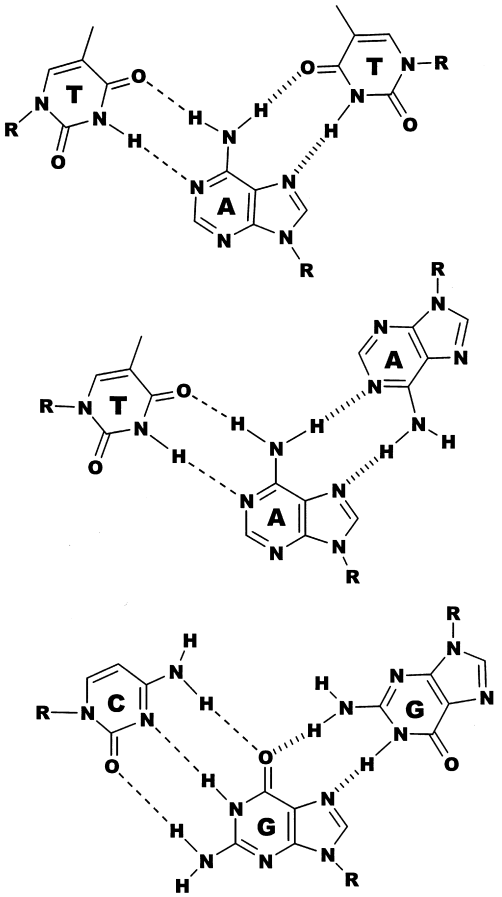

Fig. 1. T·A*T (top), T·A*A (middle) and C·G*G (bottom) DNA base triplets containing both Watson–Crick (dashed line) and Hoogsteen type (hatched line) H-bonds.

3.1. $CGCA_8CGC / GCGT_8GCG / T_8$ sample

3.1.1. NMR

Fig. 2a shows the imino proton region of NMR spectra of a 1:1 solution of $d(CGCA_8CGC)$ and $d(GCGT_8GCG)$ and Fig. 2b shows a 1:1:1 solution of $d(CGCA_8CGC)$, $d(GCGT_8GCG)$ and $d(T)_8$, in the presence of 100 mM NaCl in both cases. In the absence or presence of the third strand they look identical displaying 8 T imino proton resonances (13.6–14.3 ppm) arranged from

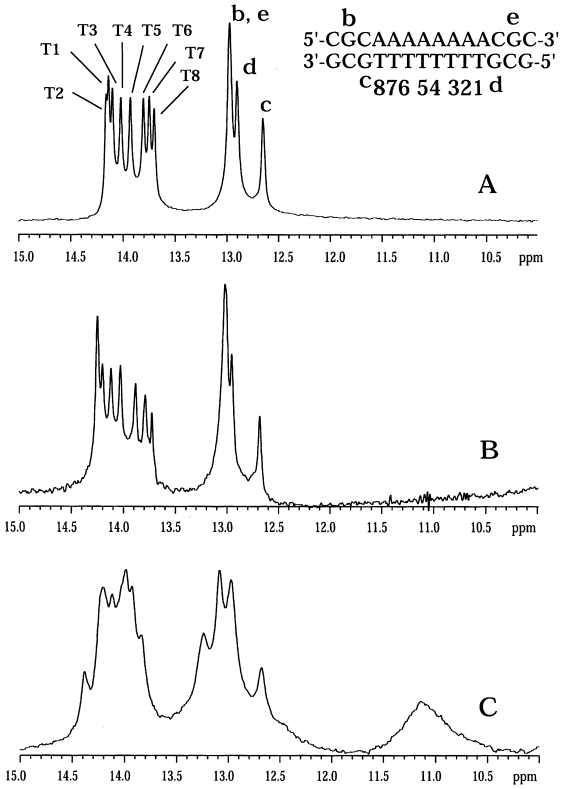

Fig. 2. Imino proton NMR spectra of a 1:1 solution of d(CGCA$_8$CGC) and d(GCGT$_8$GCG) (a) and 1:1:1 solutions of d(CGCA$_8$CGC), d(GCGT$_8$GCG) and d(T)$_8$ (b,c). Experiments were done in 10 mM phosphate buffer (pH 7.2) containing 100 mM NaCl (a,b) and 100 mM NaCl plus 50 mM $MgCl_2$ (c) in 10% D_2O/90 %H_2O at 20°C (a), 11°C (b) and 1°C (c). DNA concentration is 2 mM in each strand. The resonance assignment has been done according to Wärmländer et al. [8].

the 5′ end to 3′ end, as indicated in the figure. There are also three resonances assigned to the G imino protons (12.5–13.1 ppm). The sequential assignment is taken from our earlier study on this sequence [8].

When 50 mM $MgCl_2$ was added to the 1:1:1 solution and the temperature was lowered to 1°C, all resonances became broadened and somewhat shifted (Fig. 2c). Therefore the possibility that some minor new resonances may have appeared cannot be excluded. However, at this temperature a new broad resonance appeared at 11.15 ppm (Fig. 2c). We conclude that the third strand d(T)$_8$ remains in single strand form. The broad resonance at 11.15 ppm can be assigned to the T imino protons of the unbound third strand d(T)$_8$. This resonance shows up at 1°C (Fig. 2c), but was not visible at 11°C (Fig. 2b) due to the fast exchange of the T imino protons with solvent at this temperature.

3.1.2. CD

Fig. 3 compares the CD spectrum of a 1:1:1 solution of d(CGCA$_8$CGC), d(GCGT$_8$GCG) and d(T)$_8$ with an appropriate normalized sum of two CD spectra of a 1:1 solution of d(CGCA$_8$CGC) and d(GCGT$_8$GCG) and a solution of d(T)$_8$ recorded separately under identical experimental conditions (100 mM NaCl and 50 mM $MgCl_2$). We did not observe any significant change in terms of spectral shape, bandwidth or peak positions between the experimental spectra and the normalized sum. This is particularly clear from the difference spectrum (Fig. 3b), which is very close to the baseline. This observation indicates that the third strand remained in the unbound form under this solvent condition and further supports the NMR results of an unbound T$_8$ strand described above.

3.2. GGGA$_8$GGG / CCCT$_8$CCC / T$_8$ sample

In this sample the sequence was changed to one where the A$_8$ segment has G as its closest neighbor on both sides instead of C. This was done to probe whether the nature of the A-tract junctions (GpA and ApG as compared with CpA and ApC) influences the ability of the flanked A$_8$ segment to form a triple helix.

3.2.1. NMR

Fig. 4 shows the imino proton region of NMR spectra of a 1:1 solution of d(GGGA$_8$GGG) and d(CCCT$_8$CCC) (Fig. 4a) and a 1:1:1 solution of d(GGGA$_8$GGG), d(CCCT$_8$CCC) and d(T)$_8$ (Fig. 4b) at 5°C in the presence of 100 mM NaCl in both the cases. In Fig. 4c we observe 8 T (13.7–14.5 ppm) and 5 G (12.6–13.4 ppm) imino proton resonances corresponding to the W–C base pairing of the duplex. There is also a small broad resonance at 10.9 ppm. In Fig. 4b, addition of the third strand d(T)$_8$ does not at all affect the

imino proton resonance pattern of the W–C base-paired duplex in the range of 12.6–14.5 ppm. At approximately 11.15 ppm a very broad resonance appeared in the region of 10.3–11.9 ppm. Addition of 20 mM (Fig. 4c) and 50 mM $MgCl_2$ (Fig. 4d) caused broadening and diminishing intensity of all the resonances, but no new resonances appeared. Like the sequence where Cs flank the A_8 segment, with this sample also there was no evidence of triplex formation, even at high Mg^{2+} concentrations.

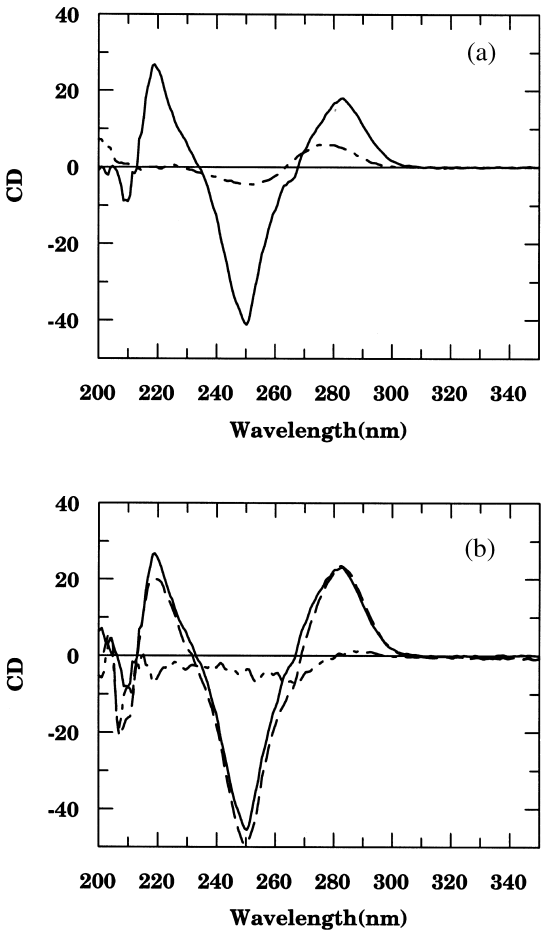

Fig. 3. (a) CD spectra of a 1:1 solution of d(CGCA$_8$CGC) and d(GCGT$_8$GCG) (—) and a solution of d(T)$_8$ (–·–·–). (b) CD spectrum of a 1:1:1 solution of d(CGCA$_8$CGC), d(GCGT$_8$GCG) and d(T)$_8$ (—) compared with the normalized sum (– – –) of the two separate CD spectra of a 1:1 solution of d(CGCA$_8$CGC) and d(GCGT$_8$GCG) and a solution of d(T)$_8$. The difference (–·–·–) between the experimental and the calculated spectra is also shown (b). The CD experiments were done in 10 mM Phosphate buffer (pH 7.2), containing 100 mM NaCl and 50 mM $MgCl_2$ at 5°C. The DNA concentration is 6 μM in each strand.

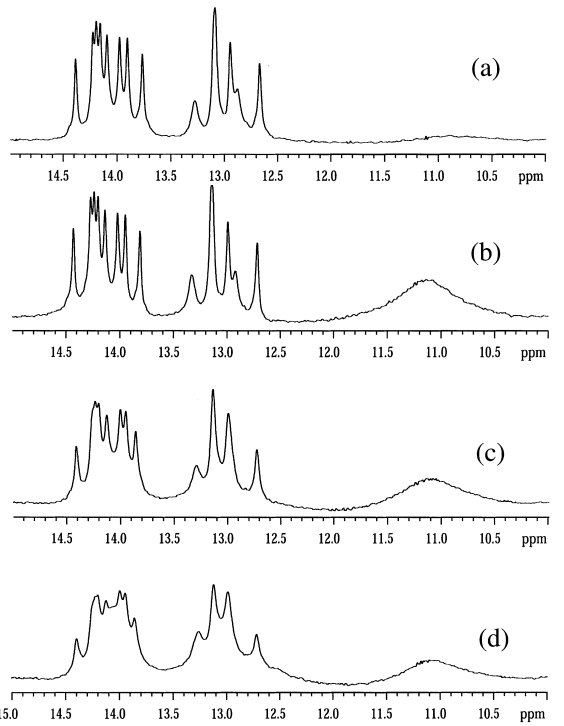

Fig. 4. Imino proton NMR spectra of a 1:1 solution of d(GGGA$_8$GGG) and d(CCCT$_8$CCC) (a) and 1:1:1 solutions of d(GGGA$_8$GGG), d(CCCT$_8$CCC) and d(T)$_8$ (b–d). Experiments were done in 10 mM phosphate buffer (pH 7.2) containing 100 mM NaCl (a, b), 100 mM NaCl plus 20 mM $MgCl_2$ (c) and 100 mM NaCl plus 50 mM $MgCl_2$ (d) in 10% D_2O/90% H_2O at 5°C. DNA concentration is 1 mM in each strand for all cases.

CD studies (data not shown) gave results very similar to those observed with the sample containing the C-flanked A_8 segment, supporting the NMR observations of absence of triplex formation.

3.3. $A_8/2T_8$ sample

In this sample the flanking GC sequences were removed from the A_8/T_8 segment, to probe the effect of the flanking base pairs to the A-tract.

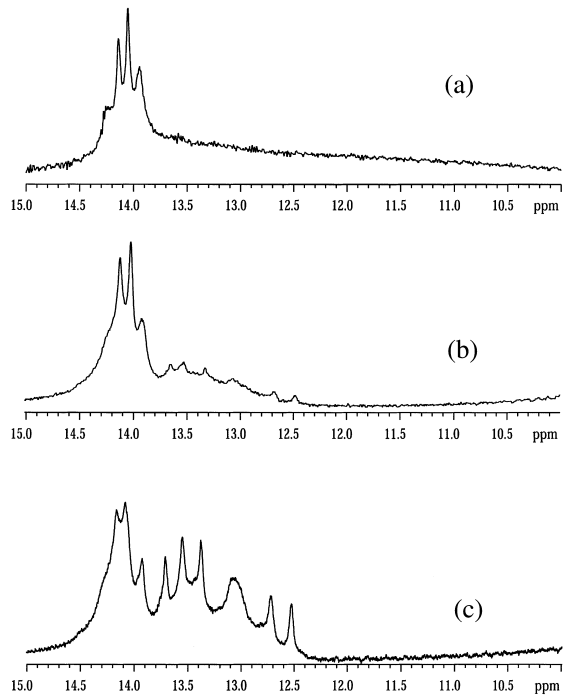

Fig. 5. Imino proton NMR spectra of 1:1 solutions (a,b) and a 1:2 solution (c) of $d(A)_8$ and $d(T)_8$. Experiments were done in 10 mM phosphate buffer (pH 7.2), 1 mM EDTA, without any added salt (a) and containing 100 mM NaCl (b,c) in 10% D_2O/90% H_2O at 1°C (a), 5°C (b) and 10°C (c). DNA concentration is 2 mM in $d(A)_8$ strand for all cases.

3.3.1. NMR

Fig. 5a,b shows the imino proton region of NMR spectra of 1:1 solutions of $d(A)_8$ and $d(T)_8$ monitored without any added salt and with 100 mM NaCl, respectively. Without salt it exhibits 4 T imino proton resonances engaged in W–C base pairing of the $A_8 \cdot T_8$ duplex in the region of 13.8–14.5 ppm. This duplex is not stable beyond 1°C (data not shown), because the screening of charges is provided by the cations from the buffer only. Addition of 100 mM NaCl to the 1:1 stoichiometric solution (Fig. 5b) partly induces some new resonances (although small) occupying a region of 12.4–13.76 ppm, on the upfield side of the W–C resonances. All the resonances become slightly broadened at the same time. These resonances are observable at a somewhat higher temperature (5°C).

With 1:2 stoichiometry and 100 mM NaCl (Fig. 5c) there are six additional resonances in the region of 12.4–13.82 ppm. These new resonances are assigned to the H-bonded imino protons involved in Hoogsteen type base pairing in a $T_8 \cdot A_8 * T_8$ motif. The resonances assigned to the W–C base pairs remain more or less unchanged except for some broadening. The triplex is stable at 10°C under the experimental condition and does not show any observable change in the temperature range of 7–13°C (data not shown).

3.3.2. Temperature-dependence

When the 1:2 solution of $d(A)_8$ and $d(T)_8$ at 100 mM NaCl was subjected to increasing temperature from 5°C to 40°C (data not shown), intensities of most of the resonances between 12.4 and 13.82 ppm were lost above 15°C, indicating that no Hoogsteen base pairs remained above that temperature.

3.4. $A_6/2T_6$ sample

In this sample the length of the A_n/T_n segment was reduced, to probe the influence of the length of the A-tract on its ability to form a triplex. Earlier studies by Umemoto et al. [9] have shown that a triplex was formed with a 1:2 solution of $d(A)_6$ and $d(T)_6$ under mild ionic conditions (100 mM NaCl).

3.4.1. NMR

Fig. 6 shows the imino proton region of NMR spectra of 1:1 and 1:2 combinations of $d(A)_6$ and $d(T)_6$ in the absence or presence of salt. With the 1:1 solution, no imino proton resonances except a very broad resonance at approximately 11.15 ppm are observable in the absence of any added salt at 1°C (Fig. 6a), indicating that the two strands are not H-bonded. The 11.15 ppm resonance should correspond to the non-H-bonded imino protons of the $d(T)_6$ strand. When NaCl is added to the 1:1 solution (Fig. 6b), or to a 1:2 solution (Fig. 6c), seven resonances are induced in the region of 12.4–14.5 ppm. This imino proton resonance pattern consisting of seven well-resolved resonances is similar in both the cases except for a slight downfield-shift of these resonances for 1:2 stoi-

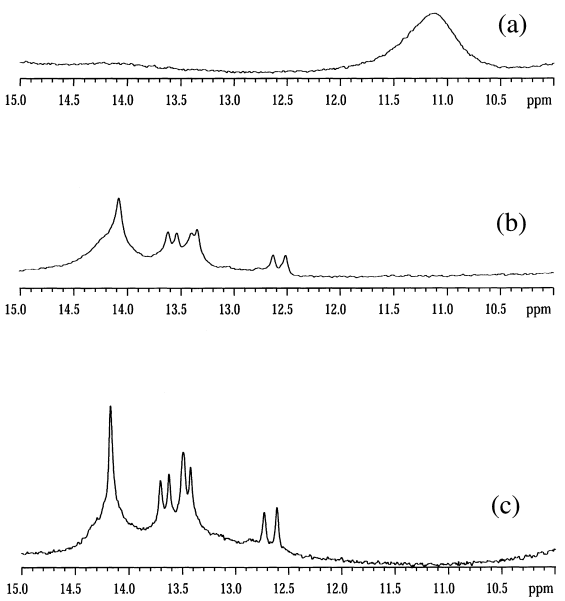

Fig. 6. Imino proton NMR spectra of 1:1 solutions (a,b) and a 1:2 solution (c) of $d(A)_6$ and $d(T)_6$. Experiments were done in 10 mM phosphate buffer (pH 7.2), without any added salt (a) and containing 100 mM NaCl (b,c) in 10% D_2O/90% H_2O at 1°C. DNA concentrations are 1 mM (a,b) and 0.5 mM (c) in $d(A)_6$ strand.

chiometric solution (Fig. 6c) with respect to those for the 1:1 stoichiometric solution (Fig. 6b). In the study of the 1:2 stoichiometric solution of $d(A)_6$ and $d(T)_6$ by Umemoto et al. [9], a very similar imino proton spectrum was assigned to a T·A∗T triplex. The lowest field resonances were assigned to the W–C base pairs, the highest field resonances were assigned to the Hoogsteen base pairs and the resonances between 13.4 and 13.8 ppm were assigned to both the W–C and the Hoogsteen base pairs. The broad resonance at 11.15 ppm observed in Fig. 6a disappeared when NaCl is added. We conclude that the 1:1 combination of $d(A)_6$ and $d(T)_6$ with no added salt remains as unbound single strands and then immediately disproportionates to a mixture of triplex + single strand even under very mild ionic conditions.

3.4.2. Temperature-dependence

We observe from the temperature-dependent NMR study of a 1:1 solution of $d(A)_6$ and $d(T)_6$ in the presence of 50 mM NaCl that between 10°C and 15°C all the resonances disappear together (data not shown). The temperature-induced melting leads directly from the triplex to single strands with no intermediate duplex stage, indicating that the triplex is more stable than the duplex in this sample (data not shown).

3.5. 2(GGGA$_8$GGG) / CCCT$_8$CCC sample

In this sample, the propensity of forming a triple helix with a Pyr·Pur∗Pur motif was probed.

3.5.1. NMR

Fig. 7a,b shows the imino proton region of NMR spectra of $d(GGGA_8GGG)$ and $d(CCCT_8CCC)$ in 1:1 and 2:1 stoichiometry, respectively, in 100 mM NaCl at 5°C. In Fig. 7a we observe 8 T (13.7–14.5 ppm) and 5 G imino

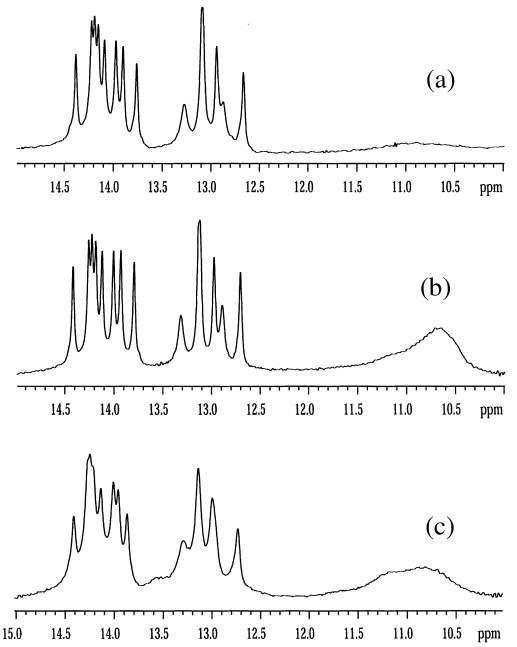

Fig. 7. Imino proton NMR spectra of a 1:1 (a) and 2:1 (b,c) solutions of $d(GGGA_8GGG)$ and $d(CCCT_8CCC)$. Experiments were done in 10 mM phosphate buffer (pH 7.2), containing 100 mM NaCl (a,b) and 100 mM NaCl plus 20 mM $MgCl_2$ (c) in 10% D_2O/90% H_2O at 5°C. DNA concentration is 1 mM in $d(CCCT_8CCC)$ strand for all cases.

proton resonances (12.6–13.4 ppm) corresponding to the W–C base pairing of the duplex. In Fig. 7b, the addition of the second purine strand under the same conditions does not at all affect the imino proton resonance pattern of the W–C base paired duplex in the range of 12.6–14.5 ppm. At approximately 10.65 ppm a very broad resonance appeared occupying the region of 10.3–11.3 ppm. As shown in Fig. 7c, addition of 20 mM $MgCl_2$ causes broadening of all the resonances without any observable change in the resonance pattern except for a very small indication of a new resonance at 13.55 ppm. A significant change of shape occurs with the broad resonance in the region of 10.5–11.5 ppm, so that it appears to be composed of two resonances of comparable intensity.

3.5.2. CD

Fig. 8 compares the CD spectrum of a 2:1 solution of d($GGGA_8GGG$) and d($CCCT_8CCC$) with an appropriate normalized sum of two CD spectra of a 1:1 solution of d($GGGA_8GGG$) and d($CCCT_8CCC$) and a solution of d($GGGA_8GGG$) recorded separately under identical experimental conditions (100 mM NaCl and 50 mM $MgCl_2$). The spectrum of 2:1 stoichiometric solution shows a small deviation from the calculated spectrum which is obvious from the difference spectrum (Fig. 8b).

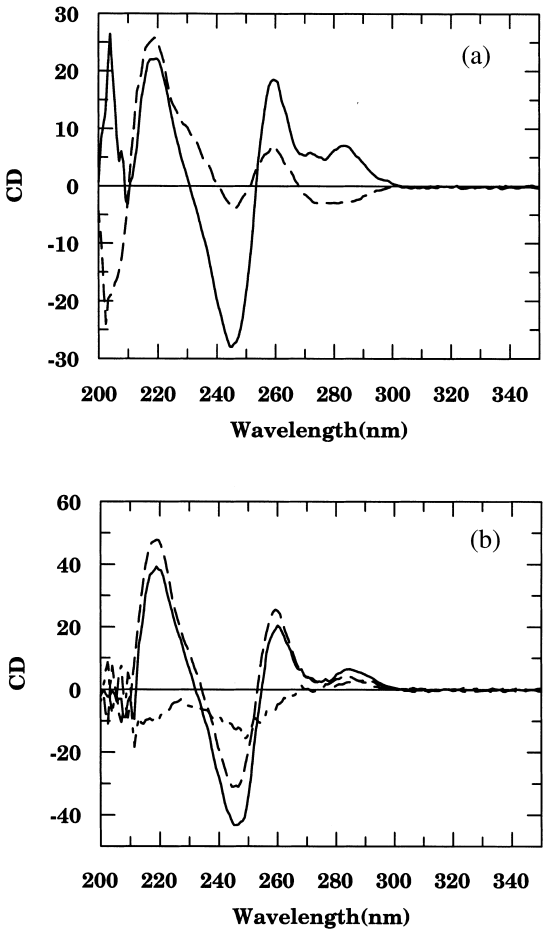

Fig. 8. (a) CD spectra of a 1:1 solution of d($GGGA_8GGG$) and d($CCCT_8CCC$) (—) and a solution of d($GGGA_8GGG$) (– – –). (b) CD spectrum of a 2:1 solution of d($GGGA_8GGG$) and d($CCCT_8CCC$) (—) compared with the normalized sum (– – –) of the two separate CD spectra of a 1:1 solution of d($GGGA_8GGG$) and d($CCCT_8CCC$) and a solution of d($GGGA_8GGG$). The difference (–·–·–) between the experimental and the calculated spectra is also shown (b). The CD experiments were done in 10 mM phosphate buffer (pH 7.2), containing 100 mM NaCl and 50 mM $MgCl_2$ at 5°C. The DNA concentration is 6 μM in d($CCCT_8CCC$) strand.

4. Discussion

As demonstrated by Wärmländer et al. [8], the 14-mer duplex $GCGT_8GCG \cdot CGCA_8CGC$ is very stable at 100 mM NaCl and 20°C. The base pair lifetimes were evaluated using a model having two exchange modes of the imino protons [8]. The base pair lifetimes corresponding to the slow mode are longer than 300 ms for the innermost A·T base pairs [8]. This is among the longest observed in any double helix up to now and should be another characteristic of so-called A-tracts. This DNA duplex exhibits well-resolved imino proton resonances (Fig. 2a) originating from the W–C base pairing. When the third strand is present in the solution in correct proportion (Fig. 2b), no new resonance appears in the region of 12.5–14.5 ppm at low temperature (11°C). Even at 50 mM Mg^{2+} concentration and 1°C temperature, this system does not form a triplex as is evident mainly from the appearance of a broad resonance at 11.15 ppm in addition to the relatively unchanged imino proton resonance pattern (Fig. 2c). The resonance at 11.15 ppm is assigned to the imino

protons of the third strand $d(T)_8$ that remains in unbound form under these solvent conditions and temperature. The absence of triplex formation in this system is fully supported by the CD observations. The inability of this duplex to accept the third strand should be connected to the anomalous structural features of its A_8/T_8 core, considered as a long A-tract.

The sample containing $d(GGGA_8GGG)/d(CCCT_8CCC)/d(T)_8$ with a GpA step instead of CpA shows a similar behavior. The common feature of these two duplex systems is that the 8-mer A-tract core is located in the midst of G·C base pairs on both sides. Obviously these systems exert a steric hindrance to the formation of Hoogsteen base pairing with a $d(T)_8$ strand as the third strand, but the inability to form a triplex does not depend on the A-tract junction being a GpA or a CpA step.

The next system studied was the 8-mer A·T segment with open ends. In Fig. 5b, the salt-induced weak resonances in the region (12.4–13.76 ppm) upfield with respect to the W–C resonances (13.8–14.5 ppm) should be assigned to the imino protons that are involved in Hoogsteen type base pairing. Although the two strands are in 50/50 proportion, addition of 100 mM NaCl shifts the equilibrium of strand association towards triplex of $T_8 \cdot A_8 * T_8$ motif to some extent. This in turn leaves some $d(A)_8$ strand unbound, whereas all $d(T)_8$ strands have been used up in complex formation. The correct stoichiometry (1:2) of the two strands in 100 mM NaCl, however, increases the intensities of these small resonances (Fig. 5c), confirming their assignment. We conclude that the 1:2 stoichiometry gives a well-developed triplex in 100 mM NaCl. The temperature-dependent study showed that the Hoogsteen base paired imino proton resonances in this sample disappeared at lower temperatures than the W–C ones, indicating that the triplex is thermally less stable than the duplex. Therefore the thermal melting is biphasic (triplex → duplex → single strand) in this case. The 1:1 stoichiometry results in a partially formed triplex at 100 mM NaCl. In the absence of any added salt, the 1:1 stoichiometry is appropriate for forming the proper duplex of the $A_8 \cdot T_8$ motif (Fig. 5a).

We interpret these observations to mean that the open-ended $A_8 \cdot T_8$ duplex exerts little steric hindrance to the third strand association, thereby indicating that the structural constraints are completely different in the two cases representing presence and absence of flanking G·C base pairs on both sides of the A-tract.

In order to investigate the length-dependence of such host $A_n \cdot T_n$ duplexes with open ends, we compared its behavior with that of a 6-mer open A·T segment. The $T_6 \cdot A_6 * T_6$ triplex imino proton spectrum was first demonstrated in a solution of 1:2 stoichiometry of A_6/T_6 by Umemoto et al. [9] with partial assignment of the resonances as described in Section 3. An additional observation of our study is that, in the presence of salt (100 mM NaCl), this A_6/T_6 system exhibits the triplex imino proton resonance pattern irrespective of the stoichiometry. Umemoto et al. [9] reported that when a well-developed triplex with 1:2 stoichiometry of A_6/T_6 is subjected to melting from 1°C to 15°C, all the imino proton resonances disappear together, indicating that the transition is monophasic and both types of H-bonds melt together. In our study, we also investigated the melting of the 1:1 stoichiometric solution, and found again that all the resonances disappear together. This means the triplex should be at least as stable as the duplex for this sequence.

Comparing A_n/T_n segments of different lengths, we conclude that in terms of the capability of duplex formation, the 6-mer A·T has less propensity than the 8-mer A·T (cf. Fig. 5a and Fig. 6a, no added salt), whereas in terms of capability of triplex formation, the 6-mer A·T has a higher propensity than the 8-mer A·T (cf. Fig. 5b and Fig. 6b, 100 mM NaCl).

For longer A_n/T_n segments Pilch et al. [10] have reported that formation of the 10-mer $T_{10} \cdot A_{10} * T_{10}$ triple helix requires either 2 M monovalent cation (Na^+) or 10 mM divalent cation (Mg^{2+}), i.e. this system requires higher cation concentration than is required for the shorter sequences studied here. We have observed that 100 mM NaCl is sufficient for the full formation of $T_8 \cdot A_8 * T_8$ triplex with 1:2 ratio of A_8/T_8. Comparing with polymeric deoxyribonucleotides, e.g. as reported by Sehlstedt et al. [17], a 1:2 ratio

of polydA/polydT forms a triplex at low temperatures at 100 mM NaCl concentration. Therefore, the stability of an oligo $T_8 \cdot A_8 * T_8$ triplex seems to be comparable to a polydT·polydA*polydT triplex under the applied conditions of DNA concentration and temperature.

In Table 1 our observations are compared with the other triplex systems reported by other research groups. It is shown in the table that an 8-mer A-tract when flanked by G·C base pairs is unable to form triplex with the third $d(T)_8$ strand even at a high divalent cation concentration, but it is an efficient partner in triplex formation when open at both ends. Our results also show that when the third strand contains Ts or Gs, the absence of a triplex structure can be probed by the observation of a broad resonance at approximately 11 ppm at low temperatures which corresponds to the unbound third strand.

The results turn out to be slightly different with the other triplet family of $T_8 \cdot A_8 * A_8$ motif. When the A_8/T_8 tract is flanked by G·C base pairs, the indications of triplex formation with another $d(GGGA_8GGG)$ strand are weak but not absent in our study (Fig. 7 and Fig. 8). We conclude that the Pyr·Pur*Pur motif requires less ionic driving force than the Pyr·Pur*Pyr motif with the same 8-mer A-tract core. With a lower number of A/T bases, e.g. with a tetramer A-tract placed in the middle of G·C base pairs, it has been reported to successfully form a triplex of $T_4 \cdot A_4 * A_4$ motif at 14 mM Mg^{2+} [11].

From the comparison of our data with those reported in the literature [9–11] we conclude that the shorter A-tracts have a higher propensity for triplex formation than the longer ones, either with the G·C base pair-flanked A-tracts of Pyr·Pur*Pur motif or with the open ended A-tracts of Pyr·Pur*Pyr motif.

The structural basis of A-tract bending has been extensively discussed [5] and reviewed [1]. It seems most likely that structural features associated with the bending of an A-tract are also related to its inaccessibility as a host duplex for triple helix formation. Particularly, two structurally anomalous phenomena have been reported for so-called A-tracts. One is the minor groove narrowing in the 5′ to 3′ direction and the increased base pair propeller twist. Another is the possible sequence-specific binding of monovalent as well as divalent cations, which has been suggested to be related to the bending of A-tracts [6].

Table 1
Conditions for duplex and triplex formation with oligonucleotides[a]

DNA	Conditions for duplex	Conditions for triplex	References
$CGCA_8CGC/GCGT_8GCG$ (1:1)	100 mM NaCl	–	This study
$CGCA_8CGC/GCGT_8GCG/T_8$ (1:1:1)	–	Not found at/below 100 mM NaCl + 50 mM $MgCl_2$	This study
$GGGA_8GGG/CCCT_8CCC$ (1:1)	100 mM NaCl	–	This study
$GGGA_8GGG/CCCT_8CCC/T_8$ (1:1:1)	–	Not found at/below 100 mM NaCl + 50 mM $MgCl_2$	This study
A_8/T_8 (1:1)	No added salt	–	This study
$A_8/2T_8$ (1:2)	–	100 mM NaCl	This study
A_6/T_6 (1:1)	Duplex not found	–	This study
$A_6/2T_6$ (1:2)	–	100 mM NaCl	[9]
A_{10}/T_{10} (1:1)	No added salt	–	[10]
$A_{10}/2T_{10}$ (1:2)	–	2 M NaCl or 10 mM $MgCl_2$	[10]
$GGGA_8GGG/CCCT_8CCC$ (2:1)	–	Partial formation in 100 mM NaCl + 50 mM $MgCl_2$	This study
$GGGA_4GGG/CCCT_4CCC$ (1:1)	No added salt[b]	–	[11]
$GGGA_4GGG/CCCT_4CCC$ (2:1)	–	14 mM $MgCl_2$[b]	[11]

[a] Sodium phosphate buffer (10 mM; pH 7.2), temperature close to 0°C.
[b] Sodium phosphate buffer (15 mM; pH 7.2), temperature 35°C.

In the review by Crothers [1], he described a 'junction model' consisting of bent A-tracts and normal straight B-DNA segments. When long A-tracts are involved, as with $CGCA_8CGC \cdot GCGT_8GCG$ and $GGGA_8GGG \cdot CCCT_8CCC$, they may deviate so much from the canonical B or B′-form that they become inaccessible or unavailable for the Hoogsteen type H-bond formation. Only when the so-called junctions are removed or the A-tracts are made shorter, the duplex allows formation of Hoogsten type H-bonds in the major groove.

The absence of triplex formation by $d(T)_8$ with either of the duplexes $CGCA_8CGC \cdot GCGT_8GCG$ or $GGGA_8GGG \cdot CCCT_8CCC$ might in principle also be caused by unfavorable free energy at the duplex–triplex junctions rather than the A-tract features. This interpretation is, however, quite unlikely in view of previous reports [22–25] where shorter DNA pyrimidine oligonucleotides (6–14 nucleotides in length) recognize particular target sequences on longer duplex DNA molecules to form triple helices with 5′ and 3′ duplex-triplex junctions. None of these target sequences contain A-tracts longer than 6-mer. The overall conclusion is that duplex–triplex junctions are not decisive for the inability of triplex formation, which instead is closely related to the presence of a long A-tract in the target sequence.

We propose a possible explanation of the observations in our study in terms of the resulting alterations of the groove dimensions. A typical feature of the A-tracts is known to be the narrowing of the minor groove [1]. When the dimensions of the minor groove changes, those of the major groove cannot remain unaltered. In the narrowed minor groove, purine N7 attached to the sugar and the C=O (guanine and thymine) or NH_2 (adenine) come closer to each other. The geometry of the major groove on the other side of the helix axis thereby changes in such a way that it becomes too wide to make favorable H-bonds with the third strand properly. It is apparent that this phenomenon occurs only when the A/T segment is of a certain length and/or flanked by G·C base pairs. The inability to support a triplex may be considered as a probe of this altered geometry. The altered ability of interaction with a third strand may also be important for the specific interaction of this type of sequences with proteins.

Acknowledgements

We wish to thank Sebastian Wärmländer and Mikael Leijon for initial help regarding the NMR experiments. This study was supported by grants from the Swedish Natural Science Research Council and the Swedish Foundation for the Strategic Research.

References

[1] D.M. Crothers, Z. Shakked, DNA bending by adenine-thymine tracts, in: S. Neidle (Ed.), Oxford Handbook of Nucleic Acid Structure, Oxford University Press, Oxford, 1999.

[2] J.K. Strauss-Soukup, P.D. Rodrigues, L.J. Maher 3rd, Effect of base composition on DNA bending by phosphate neutralization, Biophys. Chem. 72 (1998) 297–306.

[3] H-M. Wu, D.M. Crothers, The locus of sequence-directed and protein-induced DNA bending, Nature (Lond.) 308 (1984) 509–513.

[4] H.S. Koo, H-M. Wu, D.M. Crothers, DNA bending at adenine-thymine tracts, Nature (Lond.) 320 (1986) 501–506.

[5] J.G. Nadeau, D.M. Crothers, Structural basis for DNA bending, Proc. Natl. Acad. Sci. USA 86 (1989) 2622–2626.

[6] N.V. Hud, V. Sklenar, J. Feigon, Localization of ammonium ions in the minor groove of DNA duplexes in solution and the origin of DNA A-tract bending, J. Mol. Biol. 286 (1999) 651–660.

[7] E. Gavathiotis, G.J. Sharman, M.S. Searle, Sequence-dependent variation in DNA minor groove width dictates orientational preference of Hoechst 33258 in A-tract recognition: solution NMR structure of the 2:1 complex with $d(CTTTTGCAAAAG)_2$, Nucleic Acids Res. 28 (2000) 728–735.

[8] S. Wärmländer, A. Sen, M. Leijon, Imino proton exchange in DNA catalyzed by ammonia and trimethylamine: evidence for a secondary long-lived open state of the base pair, Biochemistry 39 (2000) 607–615.

[9] K. Umemoto, M.H. Sarma, G. Gupta, J. Luo, R.H. Sarma, Structure and stability of a DNA triple helix in solution: NMR studies on $d(T)_6 \cdot d(A)_6 \cdot d(T)_6$ and its complex with a minor groove binding drug, J. Am. Chem. Soc. 112 (1990) 4539–4545.

[10] D.S. Pilch, C. Levenson, R.H. Shafer, Structural analysis of the $d(A)_{10} \cdot 2(dT)_{10}$ triple helix, Proc. Natl. Acad. Sci. USA 87 (1990) 1942–1946.

[11] D.S. Pilch, C. Levenson, R.H. Shafer, Structure, stability, and thermodynamics of a short intermolecular purine-purine-pyrimidine triple helix, Biochemistry 30 (1991) 6081–6087.

[12] I. Radhakrishnan, D.J. Patel, Solution structure of a purine-purine-pyrimidine DNA triplex containing G·GC and T·AT triplets, Structure 1 (1993) 135–152.

[13] F.B. Howard, H.T. Miles, P.D. Ross, The poly(dT)·2poly(dA) triple helix, Biochemistry 34 (1995) 7135–7144.

[14] Y. He, P.V. Scaria, R.H. Shafer, Studies on formation and stability of the $d[G(AG)_5]\cdot d[G(AG)_5]\cdot d[C(TC)_5]$ and $d[G(TG)_5]\cdot d[G(AG)_5]\cdot d[C(TC)_5]$ triple helices, Biopolymers 41 (1997) 431–441.

[15] Y. Fang, Y. Wei, C. Bai, Y. Tang, S-B. Lin, L-S. Kan, Hydrated water molecules of pyrimidine/purine/pyrimidine DNA triple helices as revealed by FT-IR spectroscopy: a role of cytosine methylation, J. Biomol. Struct. Dyn. 14 (1997) 485–493.

[16] L. Yang, M. Liu, W. Deng, C. Wang, C. Bai, L.S. Kan, Influence of 5-bromodeoxycytosine substitution on triplex DNA stability and conformation, Biophys. Chem. 76 (1999) 25–34.

[17] U. Sehlstedt, P. Aich, J. Bergman, H. Vallberg, B. Norden, A. Gräslund, Interactions of the antiviral quinoxaline derivative 9-OH-B220 {2,3-dimethyl-6-(dimethylaminoethyl)-9-hydroxy-6H-indolo-[2,3-b]quinoxaline} with duplex and triplex forms of synthetic DNA and RNA, J. Mol. Biol. 278 (1998) 31–56.

[18] R.H. Shafer, Stability and structure of model DNA triplexes and quadruplexes and their interactions with small ligands, Prog. Nucleic Acid Res. Mol. Biol. 59 (1998) 55–94.

[19] N.T. Thoung, C. Hélène, Sequence-specific recognition and modification of double-helical DNA by oligonucleotides, Angew. Chem. 32 (1993) 666–690.

[20] P.P. Chan, P.M. Glazer, Triplex DNA: fundamentals, advances, and potential applications for gene therapy, J. Mol. Med. 75 (1997) 267–282.

[21] J.-S. Sun, C. Hélène, Oligonucleotide-directed triple-helix formation, Curr. Opin. Struct. Biol. 3 (1993) 345–356.

[22] C. Escudé, C.H. Nguyen, S. Kukreti et al., Rational design of a triple helix-specific intercalating ligand, Proc. Natl. Acad. Sci. USA 95 (1998) 3591–3596.

[23] J.L. Asensio, H.S. Dosanjh, T.C. Jenkins, A.N. Lane, Thermodynamic, kinetic, and conformational properties of a parallel intermolecular triplex containing 5′ and 3′ junctions, Biochemistry 37 (1998) 15188–15198.

[24] J.L. Asensio, T. Brown, A.N. Lane, Solution conformation of a parallel DNA triple helix with 5′ and 3′ triplex-duplex junctions, Structure 7 (1999) 1–11.

[25] S. Rhee, Z-J. Han, K. Liu, H.T. Miles, D.R. Davies, Structure of a triple helical DNA with a triplex-duplex junction, Biochemistry 38 (1999) 16810–16815.